COLD SPRING HARBOR
Molecular Case Studies

RAPID CANCER COMMUNICATION

Synchronous T-lymphoblastic lymphoma and neuroblastoma in a 3-yr-old with novel germline *SMARCA4* and *EZH2* variants

Pauline Tibout,[1] Joel Livingston,[1] Nisha Kanwar,[2] Kyoko E. Yuki,[2] Adam Shlien,[2,3] Bo Ngan,[4] Meredith S. Irwin,[1,5] Daniel A. Morgenstern,[1,5] Johann Hitzler,[1,5] Anita Villani,[1,5] and Sarah Cohen-Gogo[1,3]

[1]Division of Hematology/Oncology, [2]Department of Pediatric Laboratory Medicine, The Hospital for Sick Children, Toronto, Ontario M5G 1E8, Canada; [3]Genetics and Genome Biology, The Hospital for Sick Children Research Institute, Toronto, Ontario, M5G 1E8 Canada; [4]Division of Pathology, Department of Pediatric Laboratory Medicine, Hospital for Sick Children, Toronto, Ontario M5G 1E8, Canada; [5]Department of Pediatrics, University of Toronto, Toronto, Ontario M5R 0A3, Canada

Abstract T-lymphoblastic lymphoma (T-LLy) is the most common lymphoblastic lymphoma in children and often presents with a mediastinal mass. Lymphomatous suprarenal masses are possible but rare. Here, we discuss the case of a previously healthy 3-yr-old male who presented with mediastinal T-LLy with bilateral suprarenal masses. Following initial treatment, surgical biopsy of persisting adrenal masses revealed bilateral neuroblastoma (NBL). A clinical genetics panel for germline cancer predisposition did not identify any pathogenic variants. Combination large panel (864 genes) profiling analysis in the context of a precision oncology study revealed two novel likely pathogenic heterozygous variants: *SMARCA4* c.1420-1G > T p.? and *EZH2* c.1943G > C p.(Ile631Phefs*44). Somatic analysis revealed potential second hits/somatic variants in *EZH2* (in the T-LLy) and a segmental loss in Chromosome 19p encompassing *SMARCA4* (in the NBL). Synchronous cancers, especially at a young age, warrant genetic evaluation for cancer predisposition; enrollment in a precision oncology program assessing germline and tumor DNA can fulfill that purpose, particularly when standard first-line genetic testing is negative and in the setting of tumors that are not classic for common cancer predisposition syndromes.

Corresponding author:
sarah.cohen-gogo@sickkids.ca

Ontology terms: neuroblastoma; T-cell lymphoma/leukemia

Published by Cold Spring Harbor Laboratory Press

doi:10.1101/mcs.a006286

CASE PRESENTATION

A previously healthy 3-yr-old male presented with neck swelling and was found to have a large mediastinal mass on chest X-ray. Because of concern for airway compression, he was started on methylprednisolone and then had a CT chest, which confirmed the presence of a large anterior mediastinal mass yet also revealed bilateral suprarenal masses (Fig. 1A). A percutaneous tru-cut biopsy of the anterior mediastinal mass showed sheets of lymphoid cells positive for CD1a, CD3, CD5, CD4, CD8, CD10, TdT, and BCL2, confirming T-cell lymphoblastic lymphoma (T-LLy). Treatment was started as per the institutional standard of care for T-LLy based on COG AALL 0434 (Hayashi et al. 2020). Further imaging with abdominal CT confirmed the presence of bilateral suprarenal masses (5.7 × 2.4 × 3.9 cm on the right 1.3 × 1.8 × 0.8 cm on the left) (Fig. 1B). Urine catecholamines measured at the time showed mild elevation (vanillylmandelic acid [VMA] 12.6 mmol/mol creatinine [Ref range ≤6.5 mmol/

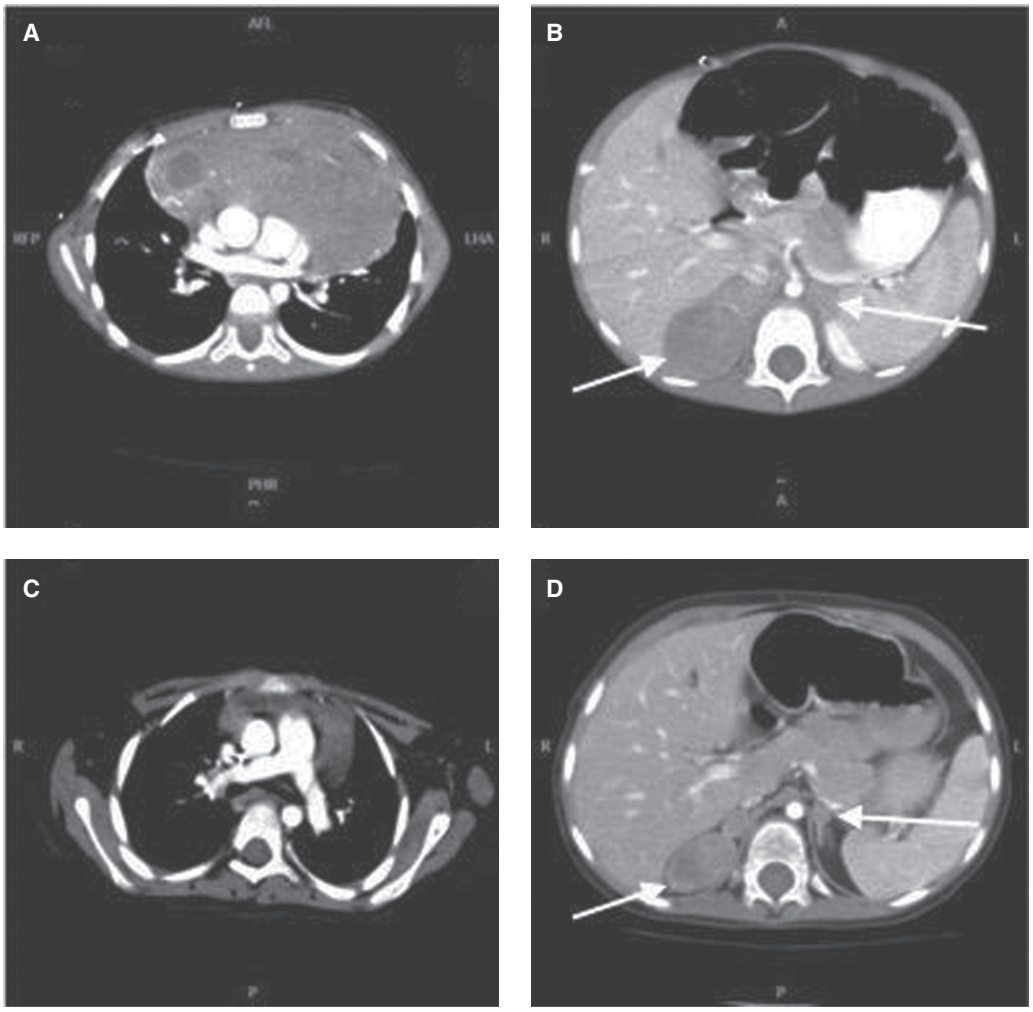

Figure 1. Axial computed tomography (CT) scan showing a large mediastinal mass at diagnosis (*A*), bilateral adrenal masses at diagnosis (*B*), significant reduction in the mediastinal mass following induction therapy (*C*), and minimal reduction in the size of the bilateral adrenal masses (*D*).

mmol creatinine]; homovanillic acid [HVA] 17.7 mmol/mol creatinine [Ref range ≤14.0 mmol/mmol creatinine]). A decision was made to continue with T-LLy therapy with repeat imaging following induction therapy.

Following the 4-wk induction phase of chemotherapy for lymphoblastic lymphoma, the anterior mediastinal showed significant reduction in size (Fig. 1C), whereas the suprarenal masses showed only minimal change (4.9 × 2.1 × 3.5 cm on right and 0.9 × 0.7 × 1 cm on left) (Fig. 1D). Repeat urine VMA and HVA were again mildly elevated but not increased from diagnosis (9.5 mmol/mol creatinine and 17.7 mmol/mol creatinine, respectively). Whole-body ^{123}I-MIBG scintigraphy showed no significant uptake in the adrenal masses or any other lesion.

Given the differential response to chemotherapy between the mediastinal and suprarenal masses, a decision was made to pursue pathological diagnosis of the suprarenal masses. A right adrenalectomy was performed via laparoscopic approach. As the mass was taking up the majority of the right adrenal gland, a partial adrenalectomy was not deemed feasible. Pathology from the right suprarenal mass showed neuroblastoma (NBL) with favorable histology by

INPC (Shimada et al. 1999) without evidence of *MYCN* amplification or 1p deletion by fluorescence in situ hybridization (FISH). With confirmed diagnoses of synchronous T-LLy and NBL, the patient was referred for cancer genetics consultation. Family history was reviewed and there was no suspicion for familial cancer predisposition. The patient was not dysmorphic; there were no cutaneous lesions including café-au-lait macules and his growth charts showed a stable 10th–20th percentile for height and weight throughout his life, with no leg length discrepancy. He had no developmental delay. A commercial germline panel for NBL and hematologic malignancy predisposition syndromes was performed and the results were negative. This panel included *ALK*, *ATM*, *BLM*, *BRCA1*, *BRCA2*, *CEPA*, *CHEK2*, *EPCAM*, *GATA2*, *HRAS*, *KIF1B*, *MLH1*, *MSH2*, *MSH6*, *NBN*, *NF1*, *PALB2*, *PHOX2B*, *PMS2*, *POT1*, *RUNX1*, *TERC*, *TERT*, and *TP53*. The patient was then enrolled in a SickKids Cancer Sequencing (KiCS) study and underwent germline and somatic next-generation sequencing (NGS) (Villani et al. 2022).

The patient completed chemotherapy for T-LLy and was followed with serial q3-mo ultrasounds for NBL surveillance until 8 yr of age. The left adrenal mass decreased in size over the following 6 mo until it was not detectable on ultrasound anymore. The right suprarenal region remained cleared after surgery. He remains disease-free 2 yr postcompletion of chemotherapy and 4 yr from initial diagnosis. The family was seen in a genetics clinic, and it was determined that the *SMARCA4* variant was paternally inherited.

TECHNICAL ANALYSIS

Briefly, the SickKids Comprehensive Cancer Panel analyzes 864 genes associated with a wide spectrum of cancer and/or an increased risk for cancer predisposition, with paired tumor–normal DNA sequencing. Tumors are sequenced using the panel and with whole-transcriptome (RNA-seq) sequencing. Genetic variants from the coding sequences and intron/exon boundaries including 10 bp of intronic sequence are investigated for the cancer panel. Copy-number changes for gene-level, whole-chromosome arm and whole chromosomes are also analyzed with NxClinical (BioDiscovery). The average sequencing depth is 1000× for germline and somatic paired analysis. Extensive methods are available in Villani et al. (2022).

GENOMIC FINDINGS

See Table 1, for genomic findings.

VARIANT INTERPRETATION

Germline DNA sequencing identified a novel heterozygous variant, c.1420-1G > T, in the *SMARCA4* gene (NM_001128849.3). This variant has not been previously reported as a benign variant or associated with any disease phenotypes in another patient. This patient was included in two previously published case series (Villani et al. 2022; Witkowski et al. 2023). This variant is absent from population controls (gnomAD database). The mutation localizes to the canonical −1 splice site, resulting in the loss of the 3′ AG splice acceptor site of intron 8. Algorithms developed to predict potential effects on splicing (SpliceSiteFinder-like, MaxEntScan, NNSplice, and GeneSplicer) predict that this variant may result in a skip of exon 9. In addition, activation of a cryptic splice site 15 bp downstream from this variant is also predicted (SpliceAI). According to The American College of Medical Genetics (ACMG) and American Molecular Pathology (AMP) guidelines (Richards et al. 2015), this novel variant was classified as likely pathogenic (PVS1, PM2_supporting).

Table 1. Genomic findings

Gene	Chr	Transcripts	HGVS DNA ref	HGVS protein ref	Variant type	Predicted effect	Allele frequency	Germline or somatic	Interpretation
SMARCA4	19	NM_001128849.1	c.1420-1G > T?	p.?	Splice acceptor	Splicing	98% in the tumor (somatic segmental loss in 19p)	Germline	Likely pathogenic
EZH2	7	NM_004456.4	c.1891delA	p.(Ile631Phefs*44)	Frameshift del	Premature truncation	50.42%	Germline	Likely pathogenic
EZH2	7	NM_004456.4	c.1943G > C (note: The *EZH2* variants are in *trans*)	p.(Gly648Ala)	Nonsynonymous SNV		40.23%	Somatic (T-LLy)	Variant of uncertain significance (VUS)
TP53	17	NM_000546.5	c.481delG	p.(Ala161Profs*9)	Frameshift del	Premature truncation	87.1% (somatic segmental loss in 17p)	Somatic (NBL)	VUS
PTEN	10	NM_000314.6	c696_699delinsTTGTCCCG	p.(Arg233Cysfs*11)	Frameshift indel	Premature truncation	13.11%–18.8%	Somatic (T-LLy)	Class 3B
PTEN	10	NM_000314.6	c.700_701insCACCAGC	p.(Arg234Profs*11)	Frameshift indel	Premature truncation	20.5%	Somatic (T-LLy)	Class 3B
NOTCH1	9	NM_017617.4	c.5162T > G	p.(Val1721Gly)	Nonsynonymous SNV	Gain of function	24.03%	Somatic (T-LLy)	VUS
BCOR	X	NM_017745.6	C.4174-2A > G	p.?	Splice acceptor	Splicing	86.11%	Somatic (T-LLy)	VUS
KMT2D	12	NM_003482.3	C.4564C > T	p.(GlN1522*)	Stopgain SNV	Loss of function	39.27%	Somatic (T-LLy)	VUS
CREBBP	16	NM_004380.2	c.4303G > A	p.(Asp1435Asn)	Nonsynonymous SNV	Loss of function	38.21%	Somatic (T-LLy)	VUS
DDX3X	7	NM_001193416.2	c.744C > T	p.(Gly248Gly)	Synonymous SNV	Splicing	43.74%	Somatic (T-LLy)	VUS

Somatic sequencing of DNA isolated from the patient's NBL tumor detected some segmental chromosomal aberrations, including one copy loss of Chromosome region 19p, which contains the *SMARCA4* gene. RNA sequencing detected usage of a cryptic splice site 15 bp downstream from the DNA variant, on the 3′ side of the canonical splice acceptor site (~75% of reads spanning this region) (Fig. 2A). Normal splicing was also detected (~25% of reads spanning this region). The level of *SMARCA4* expression was lower than that detected in other NBL samples but was not considered a statistical outlier (Fig. 2B). Immunohistochemistry (IHC) showed partial loss of SMARCA4 staining (Fig. 2C,D). This second hit was unique to the NBL, as it was not detected in the patient's lymphoma.

A distinct germline heterozygous variant, c.1891del, p.Ile631Phefs*44, was identified in the *EZH2* gene (NM_004456.5) and classified as likely pathogenic (PVS1, PM2_supporting) as per ACMG/AMP criteria. This novel variant is a frameshift mutation located in exon 16 of the *EZH2* gene, immediately upstream of the SET domain, a conserved feature of histone lysine methyltransferases. This alteration creates a premature translational stop signal, which may result in an absent or disrupted protein product. Loss of function has been described as a mechanism of oncogenicity for *EZH2*.

Somatic DNA sequencing of the T-LLy tumor identified a nonsynonymous single-nucleotide variant (SNV), c.1943G > C, p.(Gly648Ala), also occurring within the SET domain of *EZH2*, where other activating variants have been reported at hotspot locations (closest Y646) (COSMIC, OncoKb). Although gain-of-function variants are more typically observed in follicular lymphoma and diffuse large B-cell lymphomas, loss-of-function variants have

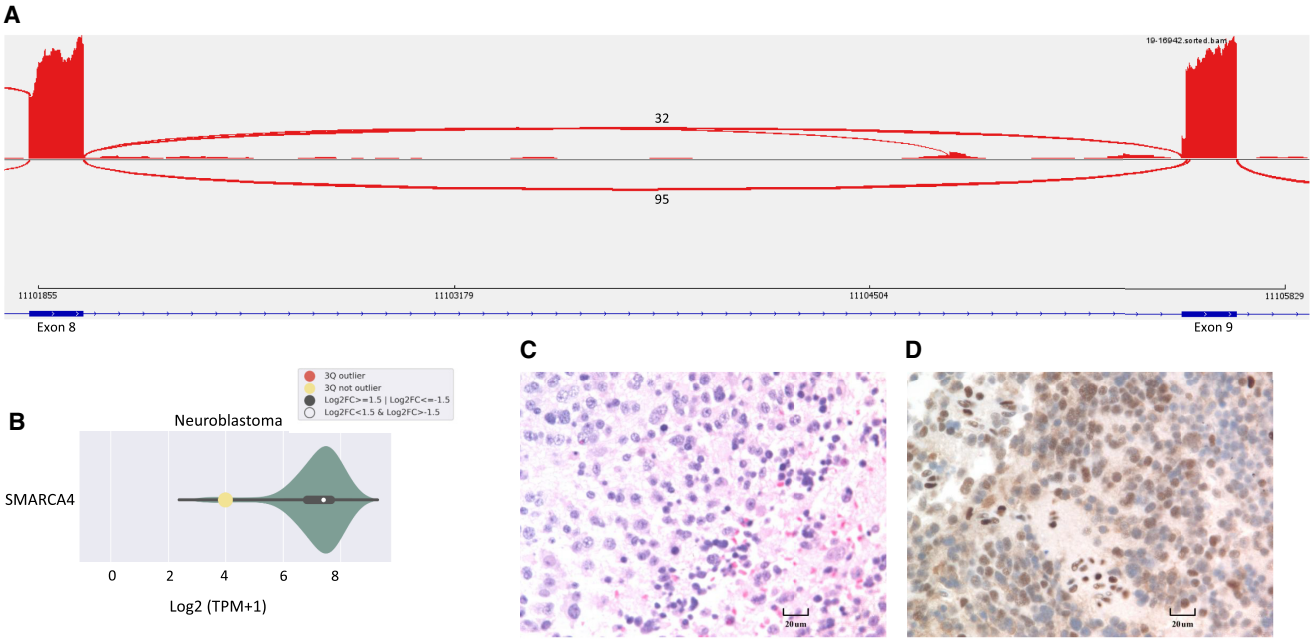

Figure 2. SMARCA4 sequencing and immunostaining. (*A*) Sashimi plot of aligned RNA sequencing data of the patient at *SMARCA4* exons 8 and 9, revealing a cryptic splice site 15 bp downstream from the DNA variant between exons 8 and 9. (*B*) Violin plot of *SMARCA4* gene expression in the neuroblastic tumor. The *x*-axis is the normalized $\log_2$ expression of *SMARCA4*. The yellow dot is the normalized expression value of *SMARCA4* in the neuroblastic tumor. (Red dot) Third quartile expression outlier, (yellow dot) not considered a third quartile expression outlier, (black dot) absolute value of $\log_2$ fold change ≥1.5, (white dot) absolute value of $\log_2$ fold change <1.5. (*C*) Pathologic findings of the adrenal mass. Hematoxylin and eosin (H&E) staining showing small round blue cells compatible with neuroblastoma (NBL) (10×). (*D*) Partial loss of SMARCA4 staining by immunohistochemistry (IHC) (10×).

been reported in T-cell ALL (PMID: 22237106). This missense variant has not been functionally characterized, so it is uncertain whether this variant is gain or loss of function. REVEL score is 0.948, which predicts this variant to be damaging. This second hit was unique to the lymphoma.

SUMMARY

Here, we discuss the case of a previously healthy 3-yr-old male, with no personal or familial history of cancer, who presented with synchronous mediastinal T-LLy and bilateral suprarenal NBL. We identified germline likely pathogenic variants in both *SMARCA4* and *EZH2*, as well as potential second hits/somatic variants in *EZH2* and a segmental loss in Chromosome 19p, encompassing *SMARCA4*, in the T-LLy and the NBL, respectively. Strikingly, SMARCA4 and EZH2 are two functional key players of their respective antagonizing chromatin remodeling complexes, SWI/SNF and PRC2 (PMID: 33230143). Loss of SMARCA4 can be used as a biomarker for the use of EZH2 inhibitor drugs, including in pediatric cancer (PMID: 37228094).

SMARCA4 is a tumor-suppressing gene that encodes BRG1, which is related to the switch/sucrose-nonfermenting (SWI/SNF) complex. BRG1 can also bind BRCA1 and regulates CD44, both actions having a role in regulating tumorigenesis (Mardinian et al. 2021). *SMARCA4* is located on chromosome region 19p13.2 (Kent et al. 2002). Somatic variants occur in 5%–7% of all malignant tumors, with a higher prevalence in small-cell carcinoma of the ovary hypercalcemic type (SCCOHT) and lung cancers (Mardinian et al. 2021). Germline pathogenic missense variants in *SMARCA4* are associated with the rare Coffin–Siris syndrome, which is characterized by dysmorphic features and developmental disabilities, without cancer predisposition (Schrier Vergano et al. 1993). Loss-of-function variants in *SMARCA4* cause the autosomal dominant rhabdoid tumor predisposition syndrome 2 (RTPS2, OMIM 613325), which is associated with early-onset rhabdoid tumors, particularly SCCOHT (Del Baldo et al. 2021). The penetrance of RTPS2 is variable, with many patients showing inheritance from an asymptomatic parent. However, somatic and/or germline pathogenic/likely pathogenic variants in *SMARCA4* have been identified previously in NBL. In a cohort sequencing study that focused on the identification of genetic alterations in chromatin remodeling genes in NBL (Bellini et al. 2019), *SMARCA4* alterations were detected in 2.5% of patients with NBL, with a frequency second only to that of *ATRX* variants, suggesting a possible role of *SMARCA4* in the development of NBL. *SMARCA4* germline variants in NBL patients were also reported in a large pediatric oncology precision medicine study (Parsons et al. 2016). Recently, Witkowski et al. (2023) reported 11 cases of heterozygous germline *SMARCA4* mutations in patients with NBL, including four previously unreported cases. Similar to our case, the alterations were predicted to encode loss of function and were associated with NBL tumors that lacked *MYCN* amplification. However, none of these cases included patients with additional synchronous or metachronous tumors.

Regarding our patient, the segmental deletion of 19p including *SMARCA4* in the NBL is a second somatic event in this gene, with corresponding partial loss of SMARCA4 on IHC, and could have contributed to the development of this tumor, adding to the evidence that this novel germline mutation is likely pathogenic. This also adds to the evidence supporting the role of *SMARCA4* in the pathogenesis of NBL. Considering cancer surveillance for germline *SMARCA4* variants, surveillance for SCCOHT was not relevant in this male patient. However, given the need for relapse surveillance in this child, as well as the evolving understanding of NBL risk in those with constitutional *SMARCA4* variants, it was decided to recommend surveillance with abdominal US every 3 mo for this patient.

EZH2 encodes the catalytic unit of Polycomb repressive complex 2 (PRC2) and has multiple functions in the regulation of gene expression, cell proliferation, apoptosis, and

senescence (Duan et al. 2020). *EZH2* dysregulation has been associated with oncogenesis, as is the case with other members of the polycomb group gene family. Overexpression of EZH2 was first described in prostate cancer (Varambally et al. 2002) and then in many other cancer types. Somatic variants with loss or gain of function in *EZH2* were discovered in some hematologic malignancies, such as lymphoma and myeloid leukemia (Duan et al. 2020). Germline variants in *EZH2* have been associated with a spectrum of overgrowth syndromes (Tatton-Brown and Rahman 1993). Some missense or truncating variants cause, with unknown penetrance, Weaver syndrome, which is characterized by hypertelorism, tall stature, macrocephaly, characteristic features, and a variable degree of cognitive disabilities (Tatton-Brown et al. 2013). Some cases of Weaver syndrome associated with leukemia, lymphoma, or NBL have been described (Coulter et al. 2008; Basel-Vanagaite 2010; Tatton-Brown et al. 2011, 2013). Our patient did have a germline likely pathogenic novel variant in *EZH2*; however, his growth followed the 15th percentile and he had no features of Weaver syndrome or overgrowth. The somatic analysis of the lymphoma showed an additional missense variant in *EZH2* that could not be functionally assessed, thus limiting our ability to conclude whether it represented a second hit contributing to the development of the patient's lymphoma.

In conclusion, synchronous cancers at such a young age warrant genetic evaluation for cancer predisposition. This case illustrates the benefits of better accessibility to precision oncology programs for children with cancer, specifically the elucidation of germline drivers not traditionally assessed by clinical candidate sequencing panels, a contribution to our knowledge of novel mechanisms of pediatric oncogenesis as well as information for future counseling and surveillance. Because both tumor types in our patient responded to upfront treatment, there was no direct therapeutic consequence of these germline and somatic findings to their treatment. However, these findings did have an important impact on future management by informing the appropriate surveillance screening for future cancer risk.

ADDITIONAL INFORMATION

Data Deposition and Access

All interpreted variants from DNA and RNA sequencing data have been deposited in the European Genome–Phenome Archive under accession codes EGAS00001006034 for RNA, EGAS00001006610 for DNA from WGS, and EGAS00001006642 for DNA sequencing from the comprehensive cancer panel. The variants have been submitted to ClinVar (https://www.ncbi.nlm.nih.gov/clinvar) under submission number SUB13819459 and accession nos. SCV004032424.1 and SCV004032425.1.

Ethics Statement

A case report does not constitute human subject research. Per SickKids policy, it therefore does not require an institutional review board (IRB) review. Informed consent was obtained from the legal guardian for the collection of clinical information and samples, as well as for the writing of a case report. Informed consent was obtained from legal guardians for participation in the KiCS precision oncology program.

Competing Interest Statement

The authors have declared no competing interest.

Received April 17, 2023; accepted in revised form October 4, 2023.

Author Contributions

P.T., S.C.-G., D.A.M., A.V., M.S.I., and J.H. provided clinical data and designed the study. All authors provided substantial contributions to the acquisition, analysis, or interpretation of data for the work. All authors wrote the draft of the manuscript or revised it critically for important intellectual content.

Funding

This work was supported by the following grants: The KiCS program is supported by the Garron Family Cancer Centre at The Hospital for Sick Children through funding from the SickKids Foundation.

REFERENCES

Basel-Vanagaite L. 2010. Acute lymphoblastic leukemia in Weaver syndrome. *Am J Med Genet A* **152A:** 383–386. doi:10.1002/ajmg.a.33244

Bellini A, Bessoltane-Bentahar N, Bhalshankar J, Clement N, Raynal V, Baulande S, Bernard V, Danzon A, Chicard M, Colmet-Daage L, et al. 2019. Study of chromatin remodeling genes implicates SMARCA4 as a putative player in oncogenesis in neuroblastoma. *Int J Cancer* **145:** 2781–2791. doi:10.1002/ijc.32361

Coulter D, Powell CM, Gold S. 2008. Weaver syndrome and neuroblastoma. *J Pediatr Hematol Oncol* **30:** 758–760. doi:10.1097/MPH.0b013e3181758974

Del Baldo G, Carta R, Alessi I, Merli P, Agolini E, Rinelli M, Boccuto L, Milano GM, Serra A, Carai A, et al. 2021. Rhabdoid tumor predisposition syndrome: from clinical suspicion to general management. *Front Oncol* **11:** 586288. doi:10.3389/fonc.2021.586288

Duan R, Du W, Guo W. 2020. EZH2: a novel target for cancer treatment. *J Hematol Oncol* **13:** 1–12. doi:10.1186/s13045-019-0838-y

Hayashi RJ, Winter SS, Dunsmore KP, Devidas M, Chen Z, Wood BL, Hermiston ML, Teachey DT, Perkins SL, Miles RR, et al. 2020. Successful outcomes of newly diagnosed T lymphoblastic lymphoma: results from children's oncology group AALL0434. *J Clin Oncol* **38:** 3062–3070. doi:10.1200/JCO.20.00531

Kent WJ, Sugnet CW, Furey TS, Roskin KM, Pringle TH, Zahler AM, Haussler D. 2002. The human genome browser at UCSC. *Genome Res* **12:** 996–1006. doi:10.1101/gr.229102

Mardinian K, Adashek JJ, Botta GP, Kato S, Kurzrock R. 2021. *SMARCA4*: implications of an altered chromatin-remodeling gene for cancer development and therapy. *Mol Cancer Ther* **20:** 2341–2351. doi:10.1158/1535-7163.MCT-21-0433

Parsons DW, Roy A, Yang Y, Wang T, Scollon S, Bergstrom K, Kerstein RA, Gutierrez S, Petersen AK, Bavle A, et al. 2016. Diagnostic yield of clinical tumor and germline whole-exome sequencing for children with solid tumors. *JAMA Oncol* **2:** 616–624. doi:10.1001/jamaoncol.2015.5699

Richards S, Aziz N, Bale S, Bick D, Das S, Gastier-Foster J, Grody WW, Hegde M, Lyon E, Spector E, et al. 2015. Standards and guidelines for the interpretation of sequence variants: a joint consensus recommendation of the American College of Medical Genetics and Genomics and the Association for Molecular Pathology. *Genet Med* **17:** 405–424. doi:10.1038/gim.2015.30

Schrier Vergano S, Santen G, Wieczorek D, Wollnik B, Matsumoto N, Deardorff MA. 1993. Coffin–Siris syndrome. In *GeneReviews* (ed. Adam MP et al.), University of Washington, Seattle. http://www.ncbi.nlm.nih.gov/books/NBK131811/

Shimada H, Ambros IM, Dehner LP, Hata J, Joshi VV, Roald B, Stram DO, Gerbing RB, Lukens JN, Matthay KK, et al. 1999. The international neuroblastoma pathology classification (the Shimada system). *Cancer* **86:** 364–372. doi:10.1002/(SICI)1097-0142(19990715)86:2<364::AID-CNCR21>3.0.CO;2-7

Tatton-Brown K, Rahman N. 1993. EZH2-related overgrowth. In *GeneReviews* (ed. Adam MP et al.), University of Washington, Seattle. http://www.ncbi.nlm.nih.gov/books/NBK148820/

Tatton-Brown K, Hanks S, Ruark E, Zachariou A, Duarte SDV, Ramsay E, Snape K, Murray A, Perdeaux ER, Seal S, et al. 2011. Germline mutations in the oncogene EZH2 cause Weaver syndrome and increased human height. *Oncotarget* **2:** 1127–1133. doi:10.18632/oncotarget.385

Tatton-Brown K, Murray A, Hanks S, Douglas J, Armstrong R, Banka S, Bird LM, Clericuzio CL, Cormier-Daire V, Cushing T, et al. 2013. Weaver syndrome and EZH2 mutations: clarifying the clinical phenotype. *Am J Med Genet A* **161:** 2972–2980. doi:10.1002/ajmg.a.36229

Varambally S, Dhanasekaran SM, Zhou M, Barrette TR, Kumar-Sinha C, Sanda MG, Ghosh D, Pienta KJ, Sewalt RG, Otte AP, et al. 2002. The Polycomb group protein EZH2 is involved in progression of prostate cancer. *Nature* **419:** 624–629. doi:10.1038/nature01075

Villani A, Davidson S, Kanwar N, Lo WW, Li Y, Cohen-Gogo S, Fuligni F, Edward L-M, Light N, Layeghifard M, et al. 2022. The clinical utility of integrative genomics in childhood cancer extends beyond targetable mutations. *Nat Cancer* **4:** 203–221. doi:10.1038/s43018-022-00474-y

Witkowski L, Nichols KE, Jongmans M, van Engelen N, de Krijger RR, Herrera-Mullar J, Tytgat L, Bahrami A, Mar Fan H, Davidson AL, et al. 2023. Germline pathogenic *SMARCA4* variants in neuroblastoma. *J Med Genet* **60:** 987–992. doi:10.1136/jmg-2022-108854